A Mixed-Integer Quadratically Constrained Programming Model for Network Reconfiguration in Power Distribution Systems with Distributed Generation and Shunt Capacitors

Pham Nang Van*, Do Quang Duy

School of Electrical and Electronic Engineering, Hanoi University of Science and Technology, Hanoi, Vietnam
*Corresponding author email: van.phamnang@hust.edu.vn

Abstract

This paper proposes a formulation based on mixed-integer quadratically constrained programming (MIQCP) for the problem of optimally determining network topology aiming at minimum power loss in electrical distribution grids considering distributed generation and shunt capacitors. The proposed optimization model is derived from the originally nonlinear optimization model by leveraging the modified distribution power flow method that is linear. This optimization model can be effectively solved by standard commercial solvers such as CPLEX. Then, the MIQCP-based formulation is verified on an IEEE 33-bus distribution network and a 190-bus real distribution network in Luc Ngan district, Bac Giang province, Vietnam, in 2021. The effects of the load demand level on optimal solutions are analyzed in detail. Furthermore, results of power flow analysis achieved from the modified distribution power flow approach are compared to those from solving nonlinear equations of power flow using the power summation method that gives exact solutions.

Keywords**:** Mixed-integer quadratically constrained programming (MIQCP), radial distribution systems, distributed generation, minimum power loss, power flow analysis.

1. Introduction

The optimization of network topology in electrical distribution systems by changing the status of sectionalizing and tie switches is commonly referred to as network reconfiguration.

Network reconfiguration can be deployed both as a planning tool and as a real-time control tool. The objective function of the network reconfiguration problem is to minimize power losses or balancing loads with the aim of achieving the radial topology of electrical distribution grids. The distribution systems are operated with the radial topology because of two main reasons: (1) to ease the coordination and protection and (2) to decrease the fault current. The optimization of network topology considering reactive power sources such as shunt capacitors can make a significant contribution to power loss minimization and better voltage profile.

The increasing integration of distributed generation (DG) into distribution networks contributes to the improvement of voltage profile, reliable enhancement of power supply and achievement of economic benefits such as minimum power losses and load balancing. The placement of distributed generation has a considerable impact on the optimal operation structure of distribution systems.

Network reconfiguration can be described as a mixed-integer nonlinear programming (MINLP) model. The techniques for solving this optimization model can be categorized into two main groups: heuristic and mathematical optimization [1]. A two-stage robust optimization formulation, which was solved by using a column-and-constraint generation algorithm for feeder reconfiguration considering uncertain loads, was proposed in [2]. The work [1] suggested a mixed-integer second-order cone programming (MISOCP) model, which exploited the second-order cone relaxation, big-M techniques and piecewise linearization to deal with a combined optimization problem of reactive power and network topology. A switch opening and exchange approach for coping with a multi-hour stochastic network reconfiguration considering the uncertainty of electricity demand and photovoltaic output was put forward in [3]. Authors in [4] introduced a discrete genetic algorithm aiming to optimize both network reconfiguration and shunt capacitors simultaneously. A hybrid particle swarm optimization technique was demonstrated in [5] to cope with the distribution grid reconfiguration problem coupled with distributed generation's reactive power control. These approaches, which were based on artificial intelligence algorithms, are time-consuming and cannot provide globally optimal solutions in most cases. The radiality constraints of the distribution system reconfiguration

problem regarding computational efficiency were proposed and verified in [6].

This research is implemented with the aim of developing a model of mixed-integer quadratically constrained programming (MIQCP) for optimally determining network topology considering distributed generation units and shunt compensators. This MIQCP model is developed by adopting a linear formulation of branch flow, the so-called Modified DistFlow (MD) for distribution systems. This work has made significant contributions as follows:

- To convert the mixed-integer nonlinear programming model of the network reconfiguration problem into the mixed-integer quadratically constrained programming model;

- To validate the MIQCP model on a real distribution system whose nodes equal 190 in Luc Ngan district, Bac Giang province, Vietnam, in 2021;

- To analyze the impact of the demand level on optimal solutions of the network reconfiguration problem.

The paper is structured into five Sections. Section 2 presents the nonlinear formulation of the optimization problem. A modified Linear DistFlow model is given in Section 3, and the MIQCP-based model of the network reconfiguration problem is presented in Section 4. Section 5 describes numerical results and discussions using an IEEE 33-bus distribution system and a 190-node real distribution grid in Luc Ngan district, and the conclusions are inferred in Section 6.

2. Nonlinear Formulation

The objective function of the optimization problem of network topology in this paper is to minimize power losses. Therefore, this objective function is described as in equation (1):

$$\min_{x_{ij},U_i,P_i,Q_i,P_{ij},Q_{ij}} \sum_{ij\in\Phi_B} R_{ij} \frac{P_{ij}^2 + Q_{ij}^2}{U_i^2} \qquad (1)$$

where x_{ij} is the binary variable involved line status; U_i stands for voltage magnitude at node i; P_i and Q_i are real and reactive power injection at node i, respectively; P_{ij} and Q_{ij} denote the active and reactive power flow at sending bus of line ij, respectively; R_{ij} is the resistance of branch ij; Φ_B is set of all branches.

The optimization problem of the grid structure encompasses the following constraints.

2.1 Binary Variable Constraints

Binary variable x_{ij} represents the switch state of line ij. If line ij is closed, then $x_{ij}=1$. Otherwise, $x_{ij}=0$.

$$x_{ij} = \{0,1\}; \quad \forall ij \in \Phi_B \qquad (2)$$

Moreover, when the line ij is open, the active and reactive powers flowing through this line have to equal zero. This requirement is expressed as in (3) that is linear inequality expressions.

$$-x_{ij}M \le P_{ij} \le x_{ij}M; \quad \forall ij \in \Phi_B$$
$$-x_{ij}M \le Q_{ij} \le x_{ij}M; \quad \forall ij \in \Phi_B \qquad (3)$$

where M is a big enough positive constant.

2.2 Power Balance Constraints

According to DistFlow [7, 8, 9], the equations of active and reactive power balance can be represented below:

$$P_{hi} = \sum_{j\in\Phi_{N(i)},j\neq h} P_{ij} + R_{hi}\frac{P_{hi}^2 + Q_{hi}^2}{U_h^2} - P_i; \quad \forall i \in \Phi_N$$

$$Q_{hi} = \sum_{j\in\Phi_{N(i)},j\neq h} Q_{ij} + X_{hi}\frac{P_{hi}^2 + Q_{hi}^2}{U_h^2} - Q_i; \quad \forall i \in \Phi_N \qquad (4)$$

$$P_i = -P_{Di} + P_{Gi}; \quad \forall i \in \Phi_N$$
$$Q_i = -Q_{Di} + Q_{Gi} + Q_{Ci}; \quad \forall i \in \Phi_N \qquad (5)$$

where Φ_N is set of all nodes; $\Phi_{N(i)}$ is the set of buses linked directly to bus i; Q_C represents reactive power injected by shunt capacitor; P_{Gi} and Q_{Gi} are real and reactive power injection by distributed generation at node i, respectively.

2.3 Voltage Equation Constraints

The voltage drop along the closed branch in distribution systems can be written as follows:

$$U_i - U_j = \frac{R_{ij}P_{ij} + X_{ij}Q_{ij}}{U_i}; \quad \forall ij \in \Phi_B \qquad (6)$$

For open branch, the method based on the big-M number is deployed to incorporate the equation of voltage constraints as below [10]:

$$-(1-x_{ij})M \le U_i - U_j \le (1-x_{ij})M; \quad \forall ij \in \Phi_B \qquad (7)$$

By combining (6) and (7), voltage equation constraints can be described using (8) and (9).

$$U_i - U_j \le (1-x_{ij})M + \frac{R_{ij}P_{ij} + X_{ij}Q_{ij}}{U_i}; \forall ij \in \Phi_B \qquad (8)$$

$$U_i - U_j \ge -(1-x_{ij})M + \frac{R_{ij}P_{ij} + X_{ij}Q_{ij}}{U_i}; \forall ij \in \Phi_B \qquad (9)$$

2.4 Line Power Flow Constraints

Bounds on real and reactive power flowing through branch ij can be represented as follows:

$$-P_{ij}^{max} \le P_{ij} \le P_{ij}^{max}; \quad \forall ij \in \Phi_B$$
$$-Q_{ij}^{max} \le Q_{ij} \le Q_{ij}^{max}; \quad \forall ij \in \Phi_B \qquad (10)$$

$$P_{ij}^2 + Q_{ij}^2 \le (S_{ij}^{max})^2; \quad \forall ij \in \Phi_B \qquad (11)$$

where $S_{ij}^{\max}$ is the thermal bound of branch ij; $P_{ij}^{\max}$ and $Q_{ij}^{\max}$ denote the capacity limits for distribution line ij, respectively. Constraints (10) can be utilized to impose not to appear the reverse power in the distribution grid by setting the lower limits to zero.

2.5 Bus Voltage Magnitude Limits

Voltage magnitude at each bus is constrained as follows:

$$U_i^{\min} \le U_i \le U_i^{\max}; \qquad \forall i \in \Phi_N \tag{12}$$

where $U_i^{\min}$ and $U_i^{\max}$ are the minimum and maximum voltage magnitudes at bus i, respectively.

2.6 Radiality Constraints

The following constraints are leveraged to impose the radial structure of distribution systems.

$$
\begin{aligned}
&\sum_{i \ne j} x_{ij} = N_N - N_{sub}; \quad \forall ij \in \Phi_B \\
&\sum_{l|r(l)=i} k_l - \sum_{l|s(l)=i} k_l = K_i; \qquad \forall i \in \Phi_N \\
&K_i = 1; \qquad \forall i \in \Phi_G \\
&K_i = 0; \qquad \forall i \notin \Phi_G \bigcup \Phi_{sub} \\
&-x_{ij} N_G \le k_{ij} \le x_{ij} N_G; \qquad \forall ij \in \Phi_B
\end{aligned}
\tag{13}
$$

where Φ_G and Φ_{sub} are the set of distributed generators (DG) and all root substations, respectively; N_G is the total number of DGs; N_{sub} is the total number of substation nodes; N_N is the total number of buses.

The above general optimization problem is a mixed-integer nonlinear programming model (MINLP). Section 3 describes a modified distribution flow (DistFlow) formulation that is linear to convert this general model into the model based on mixed-integer quadratically constrained programming (MIQCP).

3. Modified DistFlow Model

The modified DistFlow (MD) model was proposed in [11]. This MD model is linear and based on branch flow instead of bus injection. Reference [12] describes a comparative study of power flow results attained from a variety of linear power flow models, including the MD model and the nonlinear power flow model. The derivation of MD formulation is summarized as follows.

We consider a two-bus distribution grid whose equivalent circuit diagram is depicted in Fig. 1.
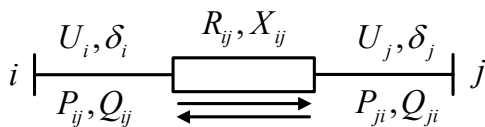
Fig. 1 A two-bus distribution system

where P_{ij} and Q_{ij} are the active and reactive power flows at the sending bus i, respectively; P_{ji} and Q_{ji} denote active power and reactive power flow at the receiving end j, respectively; U_i and U_j stand for the voltage magnitude at nodes i and j, respectively; δ_{ij} is the phase angle difference between two adjacent buses i and j; R_{ij} and X_{ij} are resistance and reactance of branch ij, respectively.

The vector diagram of voltage drop for the two-bus distribution system in Fig. 1 is shown in Fig. 2.
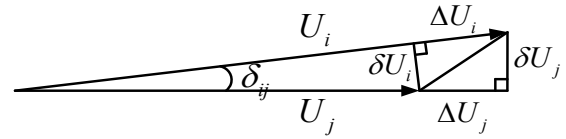
Fig. 2 The vector diagram of voltage drop

The horizontal and vertical direction components of the voltage drop are calculated using the respective expressions described below.

$$\Delta U_i = \frac{R_{ij} P_{ij} + X_{ij} Q_{ij}}{U_i}; \delta U_i = \frac{X_{ij} P_{ij} - R_{ij} Q_{ij}}{U_i} \tag{14}$$

where bus i is considered as the phase angle reference.

It is assumed that the difference between the phase angle at buses i and j can be neglected. With this assumption, the approximate formula as in (15) can be attained.

$$\sin \delta_{ij} \approx \delta_{ij}; \quad \cos \delta_{ij} \approx 1 - \frac{1}{2}\delta_{ij}^2 \tag{15}$$

From Fig. 2, the horizontal direction element of the voltage drop can be computed via (16) as follows.

$$
\begin{aligned}
\Delta U_i &= U_i - U_j \cos \delta_{ij} \approx U_i - U_j \left(1 - \frac{1}{2}\delta_{ij}^2\right) \\
\Delta U_j &= U_i \cos \delta_{ij} - U_j \approx U_i \left(1 - \frac{1}{2}\delta_{ij}^2\right) - U_j
\end{aligned}
\tag{16}
$$

To deploy the above assumption, an approximate equation is made as below.

$$\Delta U_i \approx \Delta U_j; \qquad \delta U_i = U_j \delta_{ij}; \qquad \delta U_j = U_i \delta_{ij} \tag{17}$$

By substituting (14) into (17) and leveraging the above assumption, the real and reactive powers at the sending end are related to those of the receiving end as follows:

$$\frac{P_{ij}}{U_i} \approx -\frac{P_{ji}}{U_j}; \quad \frac{Q_{ij}}{U_i} \approx -\frac{Q_{ji}}{U_j} \tag{18}$$

The power flow of branch ij at the sending end can be determined as follows:

$$P_{ij} = \frac{R_{ij}\left(U_i^2 - U_i U_j \cos\delta_{ij}\right) + X_{ij} U_i U_j \sin\delta_{ij}}{R_{ij}^2 + X_{ij}^2} \tag{19}$$

$$Q_{ij} = \frac{X_{ij}\left(U_i^2 - U_i U_j \cos\delta_{ij}\right) - R_{ij} U_i U_j \sin\delta_{ij}}{R_{ij}^2 + X_{ij}^2} \tag{20}$$

Multiplying (19) by R_{ij} and (20) by X_{ij} and using the above assumption result to the following equation:

$$U_i - U_j \approx R_{ij}\frac{P_{ij}}{U_i} + X_{ij}\frac{Q_{ij}}{U_i} \tag{21}$$

Let

$$\hat{P}_{ij} = \frac{P_{ij}}{U_i}; \quad \hat{Q}_{ij} = \frac{Q_{ij}}{U_i}; \quad \hat{P}_i = \frac{P_i}{U_i}; \quad \hat{Q}_i = \frac{Q_i}{U_i} \tag{22}$$

By employing the Taylor expansion, the following mathematical statement is obtained:

$$U^{-1} \approx 2 - U \tag{23}$$

By combining equations (21)-(23), the voltage equation of the two-bus distribution is written as follows.

$$U_j^{-1} - U_i^{-1} = R_{ij}\hat{P}_{ij} + X_{ij}\hat{Q}_{ij} \tag{24}$$

The following expressions can be obtained using $W = U^{-1}$.

$$\begin{aligned} \hat{P}_i &= P_i W_i; \quad \hat{Q}_i = Q_i W_i \\ \hat{P}_{ij} &= -\hat{P}_{ji}; \quad \hat{Q}_{ij} = -\hat{Q}_{ji} \\ W_j - W_i &= R_{ij}\hat{P}_{ij} + X_{ij}\hat{Q}_{ij} \end{aligned} \tag{25}$$

The modified DistFlow model described above is generalized using the following equations.

$$\begin{aligned} \hat{P}_{hi} &= \sum_{j\in\Phi_{N(i)}, j\neq h} \hat{P}_{ij} - \hat{P}_i; \quad \forall i \in \Phi_N \\ \hat{Q}_{hi} &= \sum_{j\in\Phi_{N(i)}, j\neq h} \hat{Q}_{ij} - \hat{Q}_i; \quad \forall i \in \Phi_N \end{aligned} \tag{26}$$

$$W_j - W_i = R_{ij}\hat{P}_{ij} + X_{ij}\hat{Q}_{ij}; \quad \forall ij \in \Phi_B \tag{27}$$

$$\begin{aligned} \hat{P}_i &= P_i W_i; \quad \forall i \in \Phi_N \\ \hat{Q}_i &= Q_i W_i; \quad \forall i \in \Phi_N \end{aligned} \tag{28}$$

It can be seen that with the MD model, the state variables to be determined in the problem of power flow analysis are the ratios of the active and reactive powers to voltage magnitude rather than these powers.

4. MIQP-Based Formulation

Deploying the modified DistFlow model represented in Section 3, the nonlinear formulation of the network reconfiguration problem is converted into the mixed-integer quadratically constrained programming as follows.

4.1 Objective Function

The object function (1) is rewritten as follows:

$$\min_{x_{ij}, W_i, U_i, \hat{P}_i, \hat{Q}_i, \hat{P}_{ij}, \hat{Q}_{ij}} \sum_{ij\in\Phi_B} R_{ij}\left(\hat{P}_{ij}^2 + \hat{Q}_{ij}^2\right) \tag{29}$$

4.2 Constraints of Binary Variables

Binary variable constraints (2)-(3) are transformed into the expressions below.

$$x_{ij} = \{0,1\}; \quad \forall ij \in \Phi_B \tag{30}$$

$$\begin{aligned} -x_{ij}M &\leq \hat{P}_{ij} \leq x_{ij}M; \quad \forall ij \in \Phi_B \\ -x_{ij}M &\leq \hat{Q}_{ij} \leq x_{ij}M; \quad \forall ij \in \Phi_B \end{aligned} \tag{31}$$

4.3 Constraints of Power Balance

Power balance constraints (4)-(5) are converted into the equations as follows.

$$\begin{aligned} \hat{P}_{hi} &= \sum_{j\in\Phi_{N(i)}, j\neq h} \hat{P}_{ij} - \hat{P}_i; \quad \forall i \in \Phi_N \\ \hat{Q}_{hi} &= \sum_{j\in\Phi_{N(i)}, j\neq h} \hat{Q}_{ij} - \hat{Q}_i; \quad \forall i \in \Phi_N \end{aligned} \tag{32}$$

$$\begin{aligned} \hat{P}_i &= -P_{Di}W_i + \hat{P}_{Gi}; \quad \forall i \in \Phi_N \\ \hat{Q}_i &= -Q_{Di}W_i + \hat{Q}_{Gi} + \hat{Q}_{Ci}; \quad \forall i \in \Phi_N \end{aligned} \tag{33}$$

4.4 Constraints of Voltage Equations

Constraints (8)-(9) are rewritten below:

$$W_j - W_i \leq \left(1 - x_{ij}\right)M + R_{ij}\hat{P}_{ij} + X_{ij}\hat{Q}_{ij}; \forall ij \in \Phi_B \tag{34}$$

$$W_j - W_i \geq -\left(1 - x_{ij}\right)M + R_{ij}\hat{P}_{ij} + X_{ij}\hat{Q}_{ij}; \forall ij \in \Phi_B \tag{35}$$

4.5 Constraints of Line Power Flow

Power flow constraints (10)-(11) are converted into the following expressions.

$$\begin{aligned} -P_{ij}^{\max}W_i &\leq \hat{P}_{ij} \leq P_{ij}^{\max}W_i; \quad \forall ij \in \Phi_B \\ -Q_{ij}^{\max}W_i &\leq \hat{Q}_{ij} \leq Q_{ij}^{\max}W_i; \quad \forall ij \in \Phi_B \end{aligned} \tag{36}$$

$$\hat{P}_{ij}^2 + \hat{Q}_{ij}^2 \leq \left(S_{ij}^{\max}W_i\right)^2; \quad \forall ij \in \Phi_B \tag{37}$$

4.6 Limits of Bus Voltage Magnitude

Constraints (12) are rewritten below.

$$2 - U_i^{\max} \leq W_i \leq 2 - U_i^{\min}; \quad \forall i \in \Phi_N \tag{38}$$

4.7 Constraints of Radial Configuration

Constraints (13) are converted into the following equations.

$$\begin{aligned} \sum_{i\neq j} x_{ij} &= N_N - N_{sub}; \quad \forall ij \in \Phi_B \\ \sum_{l|r(l)=i} k_l - \sum_{l|s(l)=i} k_l &= K_i; \quad \forall i \in \Phi_N \\ K_i &= 1; \quad \forall i \in \Phi_G \\ K_i &= 0; \quad \forall i \notin \Phi_G \bigcup \Phi_{sub} \\ -x_{ij}N_G &\leq k_{ij} \leq x_{ij}N_G; \quad \forall ij \in \Phi_B \end{aligned} \tag{39}$$

Model (29)-(39) is the MIQCP formulation and can be addressed using commercial optimization solvers such as CPLEX under GAMS [13].

5. Results and Discussions

In this section, the problem of determining the optimal topology of power distribution systems based on mixed-integer quadratically constrained programming is verified on an IEEE-33 bus distribution system [14] and a real distribution grid whose buses are equal to 190 in Luc Ngan district, Bac Giang province, Vietnam, in the year 2021. The optimization problem is solved on a 1.60 GHz i5 PC with 4 GB of RAM using CPLEX under the GAMS environment. Moreover, the power flow analysis based on the power summation method for radial power distribution systems is implemented using MATPOWER software [15] on MATLAB R2018a.

5.1 IEEE 33-bus Distribution System

We consider an IEEE 33-bus power distribution grid depicted in Fig. 3. The nominal voltage of this network is 12.66 kV. The total active and reactive powers of system demand are 3715 kW and 2300 kVAr, respectively (base scenario).

Data for lines and demands shown in Fig. 3 are depicted in [14]. In Fig. 3, the branches with solid lines are normally closed, and the branches with dashed lines are usually opened. There are four distributed generation units located in buses 18, 22, 25 and 33. The active and reactive powers of these units are assumed to be equal and set to 200 kW and 150 kVAr, respectively. Two fixed shunt capacitors are sited at nodes 18 and 33. The rated powers of these capacitors are 400 kVAr and 600 kVAr, respectively. It is assumed that the maximum and minimum nodal voltages allowed are 1.05 p.u and 0.95 p.u, respectively. The total power loss of the IEEE 33-bus system before reconfiguration for the base scenario is 84.58 kW.

Four scenarios are implemented and compared as follows:

- Scenario 1: Base scenario (the demand level is 100%).
- Scenario 2: The system loads are scaled up to 150% compared to the baseload (the demand level is 150%).
- Scenario 3: The system loads are increased to 200% compared to the baseload (the demand level is 200%).
- Scenario 4: The system loads are 2.2 times higher than the baseload (the demand level is 220%).

The branch status and computation time using the MIQCP-based model developed in Section 4 for four scenarios are shown in Table 1.

Deployment of the optimal status of branches depicted in Table 1, we do the power flow analysis to attain power loss, nodal voltages, active and reactive powers flowing through branches. The system power losses before and after reconfiguration for different scenarios are described in Table 2.

Table 1. Results of branch state and computation time for the IEEE 33-bus system

Load level	Opened branches	Time (s)
100%	7-8, 9-10, 28-29	0.315
150%	7-8, 10-11, 28-29	0.396
200%	7-8, 10-11, 28-29	2.412
220%	6-7, 10-11, 28-29	1.378

Table 2. Power loss for the 33-bus system

Load level	Power loss before reconfiguration (kW)	Power loss after reconfiguration (kW)	Power loss reduction (%)
100%	84.58	61.14	27.71
150%	238.03	165.97	30.28
200%	512.38	348.72	31.94
220%	663.21	467.46	29.52
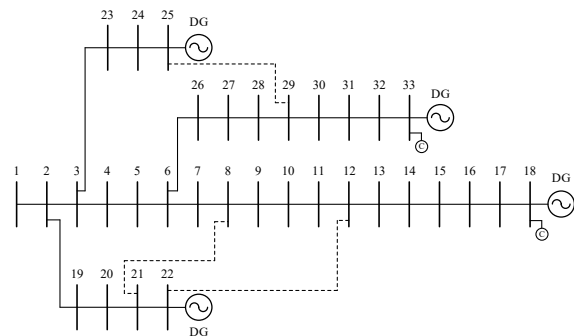
Fig. 3. IEEE 33-node distribution system

The profile of nodal voltages for the load level of 100% and 200% are sketched in Fig. 4 and Fig. 5, respectively. From Fig. 4 and Fig. 5, we can see that the network reconfiguration contributes to the enhancement of the voltage profile. In particular, for the load level of 200%, the minimum nodal voltage increases from 0.9270 p.u before network reconfiguration to 0.9612 p.u after configuration. Furthermore, the voltage profile after reconfiguration is flatter than that before reconfiguration.

The minimum voltages and average voltages of the IEEE 33-bus system for four scenarios are given in

Fig. 6 and Fig. 7, respectively. Results from Fig. 6 show that there is an increase in the minimum voltage magnitude, increasing from 0.9083 p.u before reconfiguration to 0.95 p.u after reconfiguration for the demand level of 200%. Moreover, results from Fig. 7 show that there is an increase in the average voltage magnitude, increasing from 0.9725 p.u before reconfiguration to 1.0038 p.u after reconfiguration for the demand level of 200%.
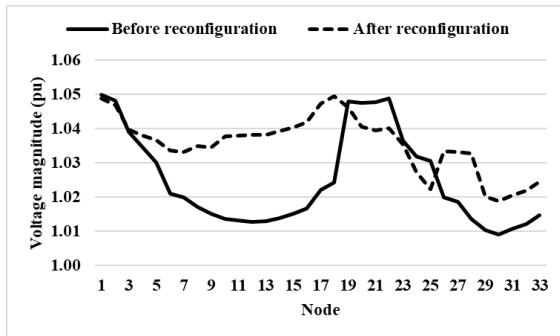
Fig. 4. Results of nodal voltages with load level of 100% for 33-bus system
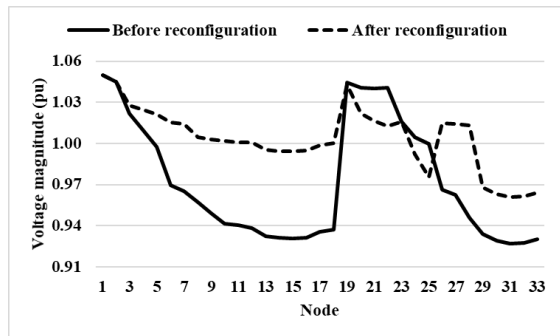
Fig. 5. Results of nodal voltages with load level of 200% for 33-bus system
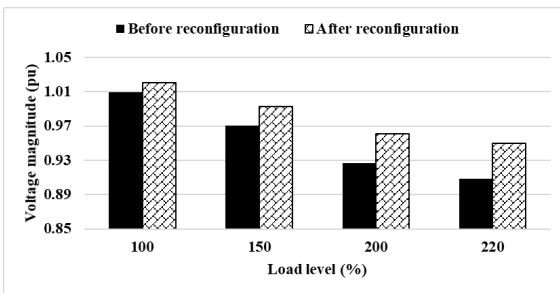
Fig. 6. Results of minimum voltage for 33-bus system
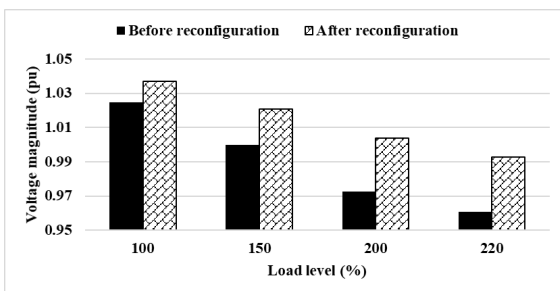
Fig. 7. Results of average voltage for 33-bus system

Table 3. Comparison of nodal voltages (p.u) for 33-bus distribution system

Node	ACPF	MIQCP	Error (%)
1	1.04876	1.04876	0.0000
2	1.04692	1.04694	0.0017
3	1.03980	1.03984	0.0037
4	1.03810	1.03814	0.0043
5	1.03669	1.03673	0.0041
6	1.03370	1.03375	0.0049
7	1.03310	1.03315	0.0049
8	1.03496	1.03523	0.0265
9	1.03449	1.03477	0.0267
10	1.03782	1.03827	0.0436
11	1.03790	1.03835	0.0437
12	1.03817	1.03862	0.0433
13	1.03827	1.03877	0.0485
14	1.03924	1.03975	0.0492
15	1.04041	1.04094	0.0506
16	1.04188	1.04241	0.0511
17	1.04726	1.04779	0.0504
18	1.04948	1.05	0.0495
19	1.04619	1.04623	0.0036
20	1.04061	1.04083	0.0212
21	1.03954	1.03981	0.0261
22	1.04022	1.04055	0.0313
23	1.03548	1.03554	0.0062
24	1.02732	1.02742	0.0100
25	1.02234	1.02247	0.0131
26	1.03343	1.03348	0.0044
27	1.03319	1.03324	0.0049
28	1.03269	1.03274	0.0046
29	1.02026	1.02041	0.0148
30	1.01884	1.01901	0.0167
31	1.02067	1.02086	0.0183
32	1.02188	1.02207	0.0184
33	1.02446	1.02465	0.0181

Table 3 describes the results of voltage magnitudes attained by solving the optimization problem based on the MD model (MIQCP) and by solving nonlinear equation systems of power flow (ACPF) for the 33-bus distribution after reconfiguration with the load level of 100%. Moreover, the total power loss achieved from deploying MIQCP and ACPF with four load scenarios is shown in Table 4. It can be seen that the errors related to nodal voltages and the total power loss of the MD model that is approximate are very small in comparison with the ACPF that is exact.

Table 4. Comparison of the total power loss (kW) for 33-bus distribution system

Load level (%)	ACPF	MIQCP	Error (%)
100	61.14	60.55	0.962
150	165.97	164.79	0.710
200	348.72	346.19	0.726
220	467.46	463.43	0.863

5.2 Luc Ngan Distribution System

This subsection describes the calculation results of the network reconfiguration problem for the electrical distribution system in Luc Ngan district, Bac Giang province, in 2021. The single-line diagram of this Luc Ngan distribution system whose nodes is equal to 190 is shown in Fig. 8.
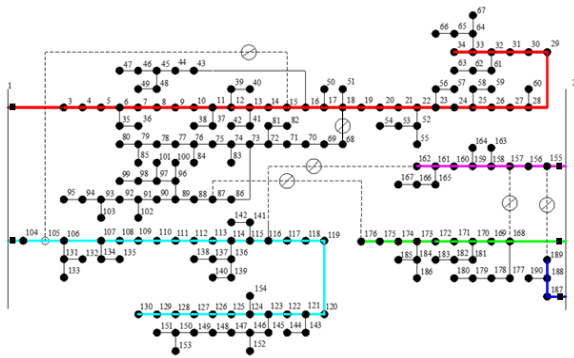
Fig. 8. Luc Ngan distibution system

The nominal voltage of the Luc Ngan distribution system is set to 35 kV. The root substations are located at buses 1 and 2. The total active and reactive powers of system demands for the base scenario (the load level of 100%) are 26,673.4 kW and 12,916.5 kVAr, respectively.

There are eleven tie switches installed in the Luc Ngan distribution network. Before network reconfiguration, five tie switches are sited at branches 15 - 105, 116 - 162, 157 - 168, 87 - 176, 155 - 189 are normally opened. Moreover, this network has seven fixed shunt capacitors placed at buses 47, 54, 66, 80, 95, 130 and 151. The respective reactive powers of these compensators are 300 kVAr, 225 kVAr, 225 kVAr, 150 kVAr, 300 kVAr, 150 kVAr and 450 kVAr. It is assumed that eight distributed generation units with the same generation output of $300 + j150$ kVA are installed at nodes 10, 22, 64, 76, 90, 110, 148 and 174.

Six scenarios with the respective demand level of 100%, 125%, 150%, 175%, 200% and 225% are carried out and analyzed.

The branch state and computation time using the MIQCP-based model developed in Section 4 for six scenarios of Luc Ngan distribution system are shown in Table 5.

Deployment of the optimal state of branches depicted in Table 5, the power flow analysis is done to achieve power loss, nodal voltages, active and reactive powers flowing through lines. The system power loss before and after reconfiguration for different scenarios are described in Table 6.

Results from Table 6 show that the total power loss of Luc Ngan grid decreases significantly after reconfiguration, a reduction of 29.44% for the load level of 200%.

Table 5. Results of branch state and computation time for Luc Ngan distribution system

Load level	Opened branches	Time (s)
100%	18-68, 1-104, 15-105, 157-168, 155-189	3.783
125%	18-68, 1-104, 15-105, 157-168, 155-189	2.843
150%	18-68, 1-104, 15-105, 157-168, 155-189	4.455
175%	18-68, 1-104, 15-105, 157-168, 155-189	2.893
200%	18-68, 1-104, 15-105, 157-168, 155-189	4.121
225%	18-68, 15-105, 116-162, 157-168, 155-189	1.533

Table 6. Power loss for Luc Ngan system

Load level	Power loss before reconfiguration (kW)	Power loss after reconfiguration (kW)	Power loss reduction (%)
100%	285.04	207.65	27.15
125%	480.50	346.77	27.83
150%	731.19	523.46	28.41
175%	1039.59	738.75	28.94
200%	1408.37	993.70	29.44
225%	1840.47	1408.40	23.48
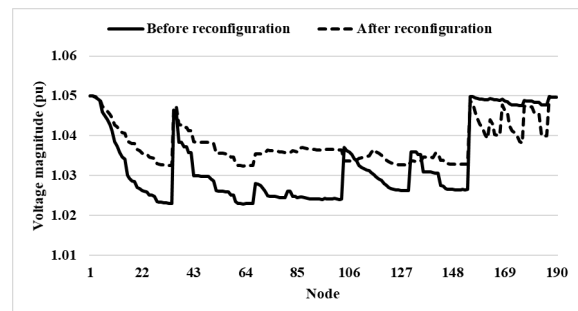
Fig. 9. Results of nodal voltages with load level of 100% for Luc Ngan distribution system
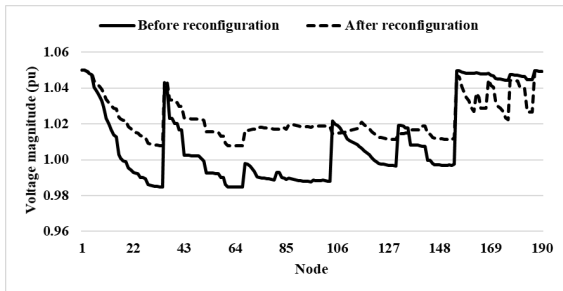
Fig. 10. Results of nodal voltages with load level of 200% for Luc Ngan distribution system
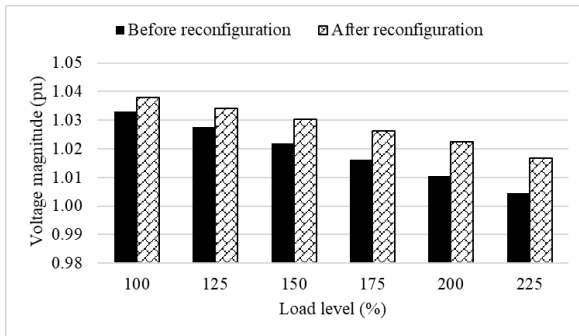
Fig. 11. Results of average voltage for Luc Ngan distribution system

The profile of nodal voltages for the load level of 100% and 200% are sketched in Fig. 9 and Fig. 10, respectively. The average voltages of Luc Ngan distribution system for six load levels are represented in Fig. 11.

From Fig. 9 and Fig. 10, we can see that the network reconfiguration contributes to enhancing the voltage profile. In particular, for the load level of 200%, the minimum nodal voltage increases from under 0.985 p.u before network reconfiguration to 1.008 p.u after configuration. Furthermore, the voltage profile after reconfiguration is flatter than that before reconfiguration.

Results from Fig. 11 illustrate that there is an increase in the average voltage magnitude, increasing from 1.011 p.u before reconfiguration to 1.022 p.u after reconfiguration for the demand level of 200%.
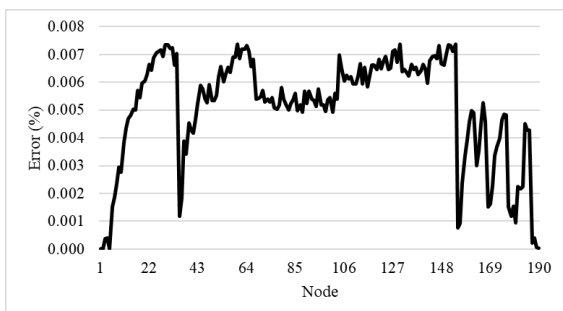
Fig. 12. Nodal voltage errors of MD model for Luc Ngan distribution system

Table 7. Comparison of the total power loss (kW) for Luc Ngan distribution system

Load level (%)	ACPF	MIQCP	Error (%)
100	207.65	207.03	0.297
125	346.77	345.93	0.241
150	523.46	522.44	0.195
175	738.75	737.57	0.159
200	993.70	992.38	0.133
225	1408.40	1406.50	0.135

Fig. 12 shows nodal voltage errors of the MD model (attained by solving the optimization problem based on MIQCP) compared to the method based on ACPF for Luc Ngan distribution system after reconfiguration with the load level of 100%. The largest error at this load level is 0.0074%, which can be neglected.

Moreover, the total power loss achieved from deploying MIQCP and ACPF with six load scenarios is shown in Table 7. It can be seen that the errors associated with the total power loss of the MD model are very small compared to the exact ACPF model.

6. Conclusion

A formulation based on mixed-integer quadratically constrained programming is developed in this paper for the optimization problem of choosing the grid structure to minimize power loss in electrical distribution grids with distributed generation units and shunt compensators. The derivation of the developed optimization model is attained from the originally mixed-integer nonlinear optimization model by adopting the linear power flow method for distribution systems, namely the MD method. The verification of the MIQCP-based formulation is executed on an IEEE 33-bus distribution network and a 190-bus real distribution network in Luc Ngan district, Bac Giang province, Vietnam, in 2021. The calculation results demonstrate that network reconfiguration considerably contributes to power loss reduction and voltage profile improvement. Furthermore, errors pertaining to nodal voltages and the total power loss achieved from the linear distribution power flow approach are very small and can be neglected in comparison with the power summation method.

References

[1] Z. Tian, W. Wu, B. Zhang, and A. Bose, Mixed-integer second-order cone programing model for VAR optimisation and network reconfiguration in active distribution networks, IET Generation, Transmission & Distribution, vol. 10, no. 8, pp. 1938-1946, May 2016,
https://doi.org/10.1049/iet-gtd.2015.1228.

[2] C. Lee, C. Liu, S. Mehrotra, and Z. Bie, Robust distribution network reconfiguration, IEEE Trans. Smart Grid, vol. 6, no. 2, pp. 836-842, Mar. 2015, https://doi.org/10.1109/TSG.2014.2375160.

[3] J. Zhan, W. Liu, C. Y. Chung, and J. Yang, Switch opening and exchange method for stochastic distribution network reconfiguration, IEEE Trans. Smart Grid, vol. 11, no. 4, pp. 2995-3007, Jul. 2020, https://doi.org/10.1109/TSG.2020.2974922.

[4] V. Farahani, B. Vahidi, and H. A. Abyaneh, Reconfiguration and capacitor placement simultaneously for energy loss reduction based on an improved reconfiguration method, IEEE Trans. Power Syst., vol. 27, no. 2, pp. 587-595, May 2012, https://doi.org/10.1109/TPWRS.2011.2167688.

[5] S. Chen, W. Hu, and Z. Chen, Comprehensive cost minimization in distribution networks using segmented-time feeder reconfiguration and reactive power control of distributed generators, IEEE Trans. Power Syst., vol. 31, no. 2, pp. 983-993, Mar. 2016, https://doi.org/10.1109/TPWRS.2015.2419716.

[6] Y. Wang, Y. Xu, J. Li, J. He, and X. Wang, On the radiality constraints for distribution system restoration and reconfiguration problems, IEEE Trans. Power Syst., vol. 35, no. 4, pp. 3294-3296, Jul. 2020, https://doi.org/10.1109/TPWRS.2020.2991356.

[7] Z. Yang, K. Xie, J. Yu, H. Zhong, N. Zhang, and Q. X. Xia, A general formulation of linear power flow models: basic theory and error analysis, IEEE Trans. Power Syst., vol. 34, no. 2, pp. 1315-1324, Mar. 2019, https://doi.org/10.1109/TPWRS.2018.2871182.

[8] J. Yang, N. Zhang, C. Kang, and Q. Xia, A state-independent linear power flow model with accurate estimation of voltage magnitude, IEEE Trans. Power Syst., vol. 32, no. 5, pp. 3607-3617, Sep. 2017, https://doi.org/10.1109/TPWRS.2016.2638923.

[9] L. Bai, J. Wang, C. Wang, C. Chen, and F. Li, Distribution locational marginal pricing (DLMP) for congestion management and voltage support, IEEE Trans. Power Syst., vol. 33, no. 4, pp. 4061-4073, Jul. 2018, https://doi.org/ 10.1109/TPWRS.2017.2767632.

[10] J. A. Taylor and F. S. Hover, Convex models of distribution system reconfiguration, IEEE Trans. Power Syst., vol. 27, no. 3, pp. 1407-1413, Aug. 2012, https://doi.org/10.1109/TPWRS.2012.2184307.

[11] T. Yang, Y. Guo, L. Deng, H. Sun, and W. Wu, A linear branch flow model for radial distribution networks and its application to reactive power optimization and network reconfiguration, IEEE Trans. Smart Grid, vol. 12, no. 3, pp. 2027-2036, May 2021, https://doi.org/10.1109/TSG.2020.3039984.

[12] P. N. Van and D. Q. Duy, Different linear power flow models for radial power distribution grids: a comparison, TNT Journal of Science and Technology, vol. 226, no. 15, pp. 12-19, Aug. 2021, https://doi.org/10.34238/tnu-jst.4665.

[13] GAMS. [Online]. Available: https://www.gams.com/

[14] S. H. Dolatabadi, M. Ghorbanian, P. Siano, and N. D. Hatziargyriou, An enhanced IEEE 33 bus benchmark test system for distribution system studies, IEEE Trans. Power Syst., vol. 36, no. 3, pp. 2565-2572, May 2021, https://doi.org/10.1109/TPWRS.2020.3038030.

[15] R. D. Zimmerman, C. E. Murillo-Sanchez, and R. J. Thomas, MATPOWER: Steady-state operations, planning, and analysis tools for power systems research and education, IEEE Trans. Power Syst., vol. 26, no. 1, pp. 12-19, Feb. 2011, https://doi.org/ 10.1109/TPWRS.2010.2051168.